UC Irvine
UC Irvine Previously Published Works

Title

Chemogenetic Manipulation of Dopamine Neurons Dictates Cocaine Potency at Distal Dopamine Transporters

Authors

Brodnik, Zachary D
Xu, Wei
Batra, Aashita
et al.

Neurobiology of Disease

Chemogenetic Manipulation of Dopamine Neurons Dictates Cocaine Potency at Distal Dopamine Transporters

Zachary D. Brodnik,[1,2] Wei Xu,[3] Aashita Batra,[1] Stacia I. Lewandowski,[4] Christina M. Ruiz,[5] Ole V. Mortensen,[4] Sandhya Kortagere,[3] Stephen V. Mahler,[5] and Rodrigo A. España[1]

[1]Department of Neurobiology and Anatomy, Drexel University College of Medicine, Philadelphia, Pennsylvania 19129, [2]National Institute on Drug Abuse, Integrative Neuroscience Research Branch, Neuronal Networks Section, Baltimore, Maryland 21224, [3]Department of Microbiology and Immunology, Drexel University College of Medicine, Philadelphia, Pennsylvania 19129, [4]Department of Pharmacology and Physiology, Drexel University College of Medicine, Philadelphia, Pennsylvania 19129, and [5]Department of Neurobiology & Behavior, University of California, Irvine, California 92697

The reinforcing efficacy of cocaine is largely determined by its capacity to inhibit the dopamine transporter (DAT), and emerging evidence suggests that differences in cocaine potency are linked to several symptoms of cocaine use disorder. Despite this evidence, the neural processes that govern cocaine potency *in vivo* remain unclear. In male rats, we used chemogenetics with intra-VTA microinfusions of the agonist clozapine-n-oxide to bidirectionally modulate dopamine neurons. Using *ex vivo* fast scan cyclic voltammetry, pharmacological probes of the DAT, biochemical assessments of DAT membrane availability and phosphorylation, and cocaine self-administration, we tested the effects of chemogenetic manipulations on cocaine potency at distal DATs in the nucleus accumbens as well as the behavioral economics of cocaine self-administration. We discovered that chemogenetic manipulation of dopamine neurons produced rapid, bidirectional modulation of cocaine potency at DATs in the nucleus accumbens. We then provided evidence that changes in cocaine potency are associated with alterations in DAT affinity for cocaine and demonstrated that this change in affinity coincides with DAT conformation biases and changes in DAT phosphorylation state. Finally, we showed that chemogenetic manipulation of dopamine neurons alters cocaine consumption in a manner consistent with changes in cocaine potency at distal DATs. Based on the spatial and temporal constraints inherent to our experimental design, we posit that changes in cocaine potency are driven by alterations in dopamine neuron activity. When considered together, these observations provide a novel mechanism through which GPCRs regulate cocaine's pharmacological and behavioral effects.

Key words: addiction; behavioral economics; dopamine neuron firing; DREADDs; fast scan cyclic voltammetry; GPCRs

---

Significance Statement

Differences in the pharmacological effects of cocaine are believed to influence the development and progression of cocaine use disorder. However, the biological and physiological processes that determine sensitivity to cocaine remain unclear. In this work, we use a combination of chemogenetics, fast scan cyclic voltammetry, pharmacology, biochemistry, and cocaine self-administration with economic demand analysis to demonstrate a novel mechanism by which cocaine potency is determined *in vivo*. These studies identify a novel process by which the pharmacodynamics of cocaine are derived *in vivo*, and thus this work has widespread implications for understanding the mechanisms that regulate cocaine consumption across stages of addiction.

Introduction

Cocaine use disorder is a neuropsychiatric condition that evolves from recreational cocaine use to compulsive, persistent, and self-destructive drug seeking and taking (Kalivas and O'Brien, 2008; Volkow and Morales, 2015). This progression is believed to stem from alterations in striatal circuit connectivity (Stuber et al., 2010; Volkow and Morales, 2015), that result from repeated co-caine-induced increases in striatal dopamine (DA) (Berke and Hyman, 2000; Kalivas and O'Brien, 2008). Cocaine increases striatal DA levels predominately through inhibition of the DA transporter (DAT) (Hurd and Ungerstedt, 1989; Kuhar et al., 1991; Chen et al., 2006), and differences in the degree of DA uptake inhibition produced by cocaine (i.e., cocaine potency) are tied to multiple behaviors associated with cocaine use disorder. For example, high cocaine potency has been linked to increases in cocaine self-administration on a limited-access schedule (Calipari et al., 2013; Siciliano and Jones, 2017), whereas long-access cocaine self-administration is believed to produce behavioral tolerance, in part, by reducing cocaine potency (Ferris et al., 2012; Calipari et al., 2013, 2014).

G-protein-coupled receptors (GPCRs) extensively regulate DA signaling, and multiple GPCRs have been proposed as potential therapeutic targets for treating cocaine use disorder (O'Brien and Gardner, 2005; Roberts, 2005; Cheer et al., 2007; Kohtz et al., 2018; Brodnik et al., 2020). We previously found that infusions of the excitatory hypocretin receptor-1 GPCR peptide into the VTA increased cocaine potency at distal DATs in the nucleus accumbens (NAc) (España et al., 2011), while intra-VTA micro-infusions of a hypocretin receptor-1 antagonist reduced cocaine potency in the NAc (España et al., 2010). In each case, effects on cocaine potency at distal DATs was observed within 20-30 min of intra-VTA GPCR manipulations. These studies open the possibility that GPCRs on DA neurons exert rapid control of cocaine potency at distal DATs.

Designer receptors exclusively activated by designer drugs (DREADDs) are genetically encoded GPCRs in which G-protein signaling is activated by exogenous molecules. In the current studies, we used DREADDs selectively expressed under the tyrosine hydroxylase (TH) promoter in TH:Cre rats to test the hypothesis that GPCRs on DA neurons exert rapid control over cocaine potency at distal DATs in the NAc, and to define the mechanism through which such changes occur. We paired chemogenetic manipulation of DA neurons with *in vitro* fast scan cyclic voltammetry (FSCV), pharmacological probes of the DAT, biochemical assessments of DAT availability and phosphorylation state, and cocaine self-administration. Our results support a novel mechanism whereby GPCR-mediated alterations in DA neuron activity impact voluntary cocaine consumption and cocaine potency via modulation of DAT conformation.

Materials and Methods

Subjects. Male, hemizygous *Long Evans-Tg3.1Deis* (TH:Cre$^+$) transgenic rats and Cre negative (Cre$^-$) WT littermates were bred at Drexel University or the University of California Irvine (Witten et al., 2011). It has been shown that cocaine sensitivity and DAT phosphorylation are generally stable in males but are influenced by the estrous cycle in female rats (Calipari et al., 2017). Thus, only male rats were used in these studies to minimize potential influences associated with the estrous cycle. Rats were housed in cages under reverse 12:12 light cycle, with free access to food and water at all times (initial surgical weight 250-400 g). All procedures were conducted in accordance with the National Institutes of Health's *Guide for the care and use of laboratory animals* under the supervision of the Institutional Animal Care and Use Committee at Drexel University and the University of California Irvine.

Chemicals and viral vectors. Zinc chloride and reagents used to make aCSF were obtained from Sigma Millipore. Cocaine hydrochloride was obtained from the National Institute on Drug Abuse drug supply program, and clozapine-n-oxide (CNO) was obtained from Tocris Bioscience. JHW 007 was synthesized and donated by Dr. Amy Hauck Newman (National Institute on Drug Abuse, Intramural Research Program). 2β-Propanoyl-3β-(4-tolyl) tropane (PTT) was donated by Dr. Huw M. L. Davies (Emory University). AAV2 vectors containing a double-floxed, inverted open reading frame (DIO) sequence for the mCherry-tagged G_i (hSyn-DIO-hM4D(Gi)-mCherry) or G_q DREADDs (hSyn-DIO-hM3D(Gq)-mCherry) were obtained from the University of North Carolina Vector Core or Addgene.

Viral transfection surgery. Rats were anesthetized with 2.0% isoflurane and then placed in a stereotaxic apparatus. Virus solutions were pressure-injected bilaterally (1 µl/hemisphere) via a Hamilton syringe connected to an infusion needle into the ventromedial midbrain over 5 min (retracted 10 min later) using the coordinates: AP, −5.5; ML, ±0.8; DV, −8.15 relative to bregma. We previously showed that this procedure results in DREADDs expression selectively in TH$^+$ neurons of the ventral tegmental area (VTA) (Mahler et al., 2019), and verified this in the current studies (Fig. 1). As controls, Cre$^-$ rats were injected with one of the same DIO vectors, although no expression was observed in any Cre$^-$ rat with either virus (Mahler et al., 2019). Rats used for intra-VTA infusions of CNO underwent a second surgery 4–5 weeks after viral infusions. Rats were anesthetized with 2.0% isoflurane, placed in a stereotaxic apparatus, and implanted with a 26 G guide cannula targeted 4 mm above the VTA: AP, 5.5; ML, ±1.9; DV, −4.3; 4° from vertical (España et al., 2010). Subjects were allowed 4-6 d to recover.

Drug administration. For FSCV and self-administration studies using systemic administration of CNO, rats were injected with a single intraperitoneal dose of 1 mg/kg in saline (total volume: 0.5–1.0 ml). For FSCV and Western blot experiments using intra-VTA administration of CNO, rats were briefly anesthetized with 1.5% isoflurane, and a 4 mm projection length, 30 G infusion needle was inserted into the guide cannula and secured in place. Subjects were allowed to fully awaken before 0.5 µl of 1 mM CNO was pressure-injected bilaterally over 2 min (retracted 5 min later). For self-administration studies, rats were gently handheld, and 0.5 µl of 1 mM CNO was microinjected bilaterally over 90 s, then injectors were left in place for an additional 60 s to allow diffusion. Microinfusions at this volume and concentration are well tolerated, exert changes in behavior in DREADDs-expressing animals, and do not produce behavioral alterations in control rats (Mahler et al., 2019).

In vitro *fast scan cyclic voltammetry procedure and analysis.* Rats were anesthetized for 3 min with 2.5% isoflurane before decapitation (Brodnik and España, 2015). Following decapitation, brains were quickly removed and transferred to ice-cold oxygenated aCSF containing the following (in mM): NaCl (126), KCl (2.5), NaH$_2$PO$_4$ (1.2), CaCl$_2$ (2.4), MgCl$_2$ (1.2), NaHCO$_3$ (25), glucose (11), L-ascorbic acid (0.4), pH adjusted to 7.4. Coronal slices containing the NAc were prepared using a vibrating tissue slicer, and then transferred into a continuously oxygenated aCSF bath at room temperature. Following a 30 min recovery period, slices were transferred to a testing chamber flushed with aCSF (32° C). A bipolar stimulating electrode was placed on the surface of the slice, and a carbon fiber microelectrode (100-200 µm length, 7 µm diameter) was placed in the lateral NAc. DA release was elicited with a single electrical stimulation pulse (400 µA, 4 ms, monophasic) every 3 min, and extracellular DA was measured at the carbon-fiber electrode every 100 ms by applying a triangular voltage waveform (−0.4 to 1.2 to −0.4 V vs Ag/AgCl, 400 V/s). Stable baseline DA release and uptake were recorded (<10% variation) before cocaine (0.3-30 µM), JHW 007 (0.3-30 µM), or PTT (0.1-10 µM) was applied at cumulatively increasing concentrations. Cocaine, JHW 007, and PTT concentrations were selected based on previous work (Bennett et al., 1995; Desai et al., 2005; John and Jones, 2007; Brodnik et al., 2017a) and preliminary slice voltammetry studies run in our laboratory (data not shown). Drug concentrations were increased when stability was reached (three stimulations with <10% variation), which occurred within 20 min for cocaine and PTT,
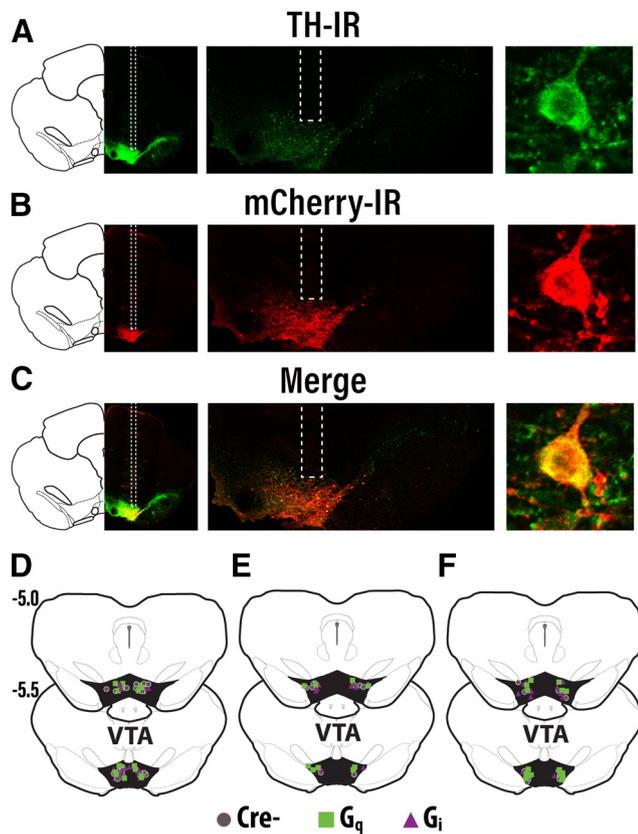
Figure 1. Verification of viral expression and cannulae placements. Representative low-, medium-, and high-resolution photomicrographs of (***A***) TH, (***B***) mCherry, and (***C***) merged with cannulae placement identified with a dotted white line. Schematic diagrams of cannulae placements for animals used in (***D***) FSCV, (***E***) Western blot, and (***F***) self-administration experiments. TH: tyrosine hydroxylase, VTA: ventral tegmental area.

and within 25 min for JHW 007. For experiments investigating the effects of Zn^{2+} on cocaine potency, we applied 30 μM cocaine; and once stability was reached (three stimulations with <10% variation), we applied a combination of 30 μM cocaine and 20 μM Zn^{2+}.

For FSCV data, evoked DA release was calculated relative to *post hoc* electrode calibrations. DA uptake was analyzed using a Michaelis-Menten–based model (Yorgason et al., 2011). Baseline uptake was determined by setting K_m values to 0.18 μM and establishing baseline V_{max} for each subject. All drug-induced alterations in uptake were attributed to changes in apparent K_m. Inhibition constants (K_i) were defined as the slope of a linear regression of K_m values across cocaine doses divided by baseline K_m (0.18 μM) (Calipari et al., 2015).

Western blot procedures and data analysis. Striatal synaptosomes were prepared and membrane fractionation was preformed using a modification of published procedures (Dunah and Standaert, 2001; Foster and Vaughan, 2011). Rats were decapitated 30 min after intra-VTA microinfusions of CNO, and the ventral striatum was rapidly dissected, weighed, and homogenized in ice-cold lysis buffer (1000 μl, 50 mM Tris-HCl, pH 7.4, 1 mM EDTA, 320 mM sucrose) with 1 $\times$ protease inhibitor cocktail, 1 $\times$ phosphatase inhibitor cocktail, and 1 mM PMSF. The homogenate was centrifuged at 1000 $\times$ g for 5 min at 4°C. The resulting supernatant was recentrifuged at 10,000 $\times$ g for 20 min at 4°C. The resulting synaptosomal pellet was resuspended with 300 μl lysis buffer for Western blot studies. Immunoblotting was performed with rabbit anti phospho-DAT polyclonal antibody (1:1000, PhosphoSolutions) or rabbit anti-DAT polyclonal antibody (1:1000, EMD Millipore) and peroxidase-conjugated goat anti-rabbit IgG (H + L) (1:5000, Jackson ImmunoResearch Laboratories). GAPDH was used as membrane protein control and determined with rabbit anti-GAPDH polyclonal antibody (1:5000, Thermo Fisher Scientific). Phosphorylated or total DAT and GAPDH immunoblots were quantified by densitometry with ImageQuant

LAS4000 (GE Healthcare Bio-Sciences). Data were analyzed and presented as ratio of phosphorylated or total DAT and GAPDH.

Self-administration procedures and economic demand analysis. Rats were trained to self-administer cocaine under a within-session cocaine demand protocol, as described previously (España et al., 2010; Oleson et al., 2011; Bentzley et al., 2013; Brodnik et al., 2017b). All sessions were short access (2 h) fixed ratio 1 schedule sessions, which have previously been shown to not alter cocaine potency at the DAT (Calipari et al., 2013). On this schedule, rats self-administered cocaine at doses that decreased in 10 min blocks over the 110 min session (383.5, 215.6, 121.3, 68.2, 38.3, 21.6, 12.1, 6.8, 3.8, 2.2, and 1.2 μg per infusion), requiring increasing effort across the session to maintain preferred brain cocaine concentrations. After every session, a demand curve was fitted to the consumption data from each rat using an exponential demand equation to determine demand for cocaine as previously described (Hursh, 1993; Bentzley et al., 2013). The values of α and Q_0 were calculated using previously described procedures (Bentzley et al., 2013). To reduce variability resulting from intra-VTA injection stress, each condition (vehicle/CNO) was repeated twice in each animal, and α/Q_0 values averaged to determine a mean value for each variable per rat. Using this behavioral economic approach, effects of neural manipulations on (1) preferred cocaine blood levels under low-effort conditions (free consumption; Q_0), and (2) the sensitivity of demand to price (demand elasticity; α) can be derived from data in a single session. Rats were trained for a minimum of 5 d, until reaching <25% variability of the α parameter in the last three sessions. Values for α and Q_0 were calculated as a percent of stable performance on the prior 3, drug-free training days.

Histology. For FSCV and Western blot experiments, the midbrain was transferred to (10% formalin) following the removal of the forebrain for experimental tissue processing. Brains remained in formalin for at least 2 d before being transferred to 20% sucrose, where they were stored at 4°C until further processing. For rats used in self-administration studies, rats were perfused with 4% paraformaldehyde, and brains were postfixed overnight in 4% PFA before being transferred to 20% sucrose.

Viral expression was verified by visualization of endogenous mCherry fluorescence. Multifluorescence immunohistochemistry was used to verify expression of mCherry and TH. Free-floating coronal sections (40 μm) were incubated in phosphate buffer (PB) containing 4% BSA and 0.3% Triton X-100. Sections were then incubated with mouse anti-mCherry (1:500, 632543, Takara Bio) and rabbit anti-TH (1:1000, AB152, Millipore) primary antibodies overnight at 4°C. Sections were then rinsed (3 $\times$ 10 min in PB) before being incubated with corresponding fluorescent secondary donkey anti-mouse (1:100 AlexaFluor-594, Jackson ImmunoResearch Laboratories) or donkey anti-rabbit (1:100 AlexaFluor-594, Jackson ImmunoResearch Laboratories), antibodies for 2 h at room temperature. Sections were then rinsed (3 $\times$ 10 min in PB) and mounted before images were collected. A representative multifluorescence photomicrograph and a schematic of cannulae placements are depicted in Figure 1.

Experimental design and statistical analysis. Data were analyzed using IBM SPSS Statistics 24 or GraphPad Prism version 5.0. Outliers were determined using Grubbs' test and removed from further analysis. Descriptions of specific features of experimental design and statistical analyses are reported in Results for each analysis.

Results

Systemic activation of G_q or G_i DREADDs on DA neurons alters cocaine potency at the DAT

We first examined whether systemic activation of G_q or G_i DREADDs expressed in DA neurons of the VTA influence cocaine potency at the DAT by measuring cocaine concentration-inhibition curves. Cre$^-$ rats that received virus infusions but do not express DREADDs were used as controls for all experiments (Mahler et al., 2019). All rats, including Cre$^-$ controls, received a single 1.0 mg/kg intraperitoneal injection of the DREADDs agonist CNO. Subjects were killed 1 h after CNO injections, and brain slices containing the striatum were prepared for FSCV
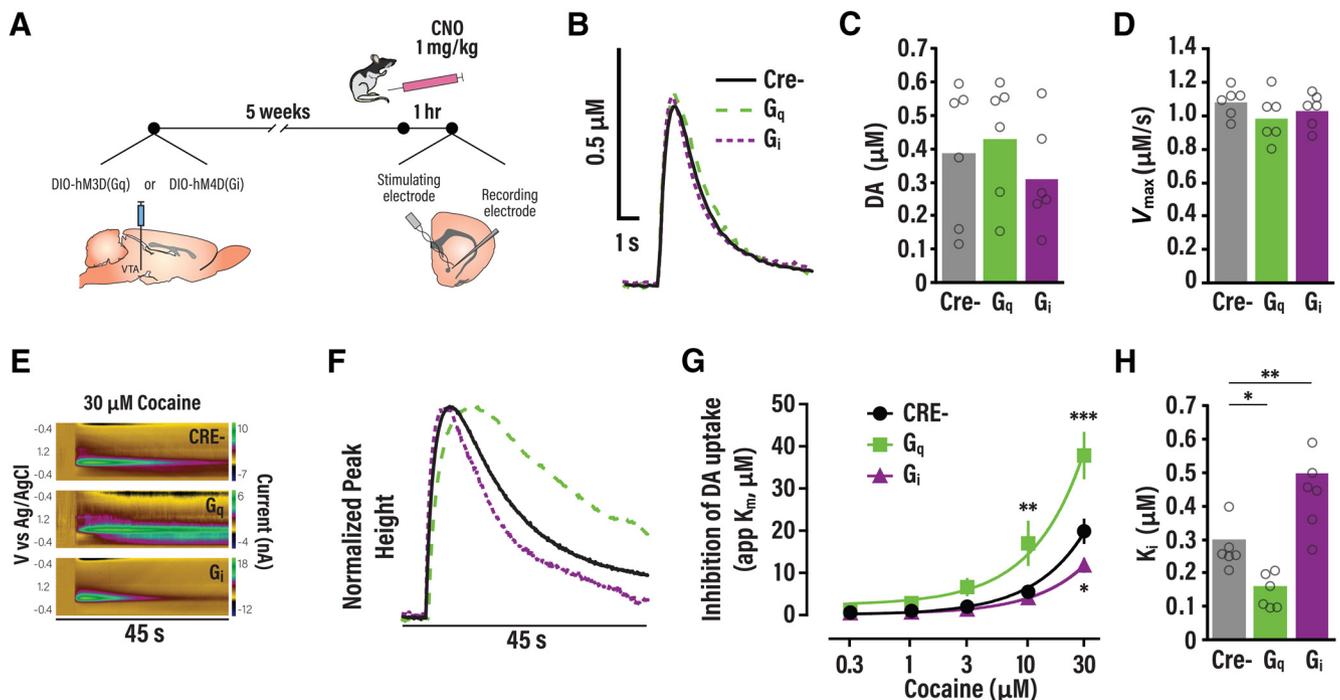
Figure 2. Activation of G_q and G_i DREADDs by systemic administration of CNO produces rapid, bidirectional changes in NAc cocaine potency. **A**, Experimental timeline. **B**, Example traces of stimulated DA release at baseline for Cre^-, Cre^+:G_q, and Cre^+:G_i rats. **C**, Average DA release at baseline. **D**, Average DA uptake rate (V_{max}) at baseline. Example (**E**) color plots and (**F**) current versus time plots of DA release and uptake in the presence of cocaine (30 μM) for Cre^-, Cre^+:G_q, and Cre^+:G_i rats. **G**, Inhibition of DA uptake following cumulative cocaine concentrations (0.3-30 μM). **H**, Average cocaine K_i. Data are mean ± SEM. $n = 6$ for all groups. Dunnett's *post hoc*: ***$p < 0.001$; **$p < 0.01$; *$p < 0.05$ versus Cre^- control.

(Fig. 2A). Baseline stimulated DA release and uptake as well as inhibition of DA uptake following cocaine (apparent K_m) were assessed (Fig. 2B–D). Activation of G_q or G_i DREADDs did not influence baseline DA release (one-way ANOVA: $F_{(2,15)} = 0.597$, $p = 0.562$) or uptake (one-way ANOVA: $F_{(2,15)} = 1.058$, $p = 0.372$). However, activation of G_q DREADDs enhanced cocaine potency (i.e., increased inhibition of DA uptake), whereas activation of G_i DREADDs reduced cocaine potency (two-way ANOVA with DREADDs group as the between-subjects measure and cocaine concentration as the repeated measure: DREADDs: $F_{(2,15)} = 10.49$, $p < 0.001$; Cocaine: $F_{(4,60)} = 93.44$, $p < 0.001$; DREADDs × Cocaine: $F_{(8,60)} = 10.34$, $p < 0.001$; Fig. 2E–G). Changes in cocaine potency corresponded with decreased cocaine K_i following activation of G_q DREADDs and increased cocaine K_i following G_i DREADDs (one-way ANOVA: $F_{(2,15)} = 19.82$, $p < 0.001$; Fig. 2H). These observations indicate that activation of G_q or G_i DREADDs in DA neurons rapidly elicits respective increases or decreases in cocaine potency.

Activation of G_i DREADDs on DA axons in the striatum reduces cocaine potency at proximal DATs

DREADDs expressed in DA neurons of TH:Cre^+ rats are localized and functional in both the somatodendritic and axonal compartments (Mahler et al., 2019). Thus, changes in cocaine potency induced by systemic injections of CNO may occur through activation of axonal and/or somatodendritic DREADDs. To address this, we examined whether activation of axonal DREADDs influences cocaine potency. We prepared brain slices from CNO naive, Cre^- control, and Cre^+:G_q or Cre^+:G_i rats and transferred slices to the recording chamber for a 30 min incubation with 1 μM CNO (in oxygenated aCSF at 32°C). It is important to note that the fiber tracts connecting the VTA to DA release sites in the NAc are severed in our slice preparation; thus,

incubation of striatal slices with CNO selectively activates axonal DREADDs. We washed off the CNO for 30 min before measuring stimulated DA release and uptake at baseline as well as the effects of cocaine using FSCV (Fig. 3A). We found that activation of G_q or G_i DREADDs with CNO incubation did not alter baseline DA release (one-way ANOVA: $F_{(2,15)} = 0.5619$, $p = 0.582$; Fig. 3B,C) or uptake (one-way ANOVA: $F_{(2,15)} = 0.454$, $p = 0.833$; Fig. 3B,D) and that activation of G_q DREADDs did not affect cocaine potency. Nevertheless, activation of G_i DREADDs significantly reduced cocaine potency (two-way ANOVA with DREADDs group as the between-subjects measure and cocaine concentration as the repeated measure: DREADDs: $F_{(2,15)} = 8.927$, $p < 0.001$; Cocaine $F_{(4,60)} = 547.7$, $p < 0.001$; DREADDs × Cocaine: $F_{(8,60)} = 11.54$, $p < 0.001$; Fig. 3E–G). Further, changes in cocaine potency corresponded with increased cocaine K_i following activation of G_i DREADDs (one-way ANOVA: $F_{(2,15)} = 13.64$, $p < 0.001$; Fig. 3H). Together, these findings demonstrate that activation of axonal G_i DREADDs is sufficient to reduce cocaine potency at the DAT, but that activation of axonal G_q DREADDs is not.

Activation of somatodendritic G_q and G_i DREADDs on DA neurons alters cocaine potency at distal DATs in the NAc

We next examined whether selective activation of somatodendritic DREADDs impacts cocaine potency at distal DATs in the NAc. We implanted bilateral cannulae targeted to the VTA of Cre^- controls, as well as Cre^+:G_q or Cre^+:G_i rats. On the day of experimentation, we inserted infusion needles and pressure-injected 0.5 μl of 1 mM CNO directly into the VTA (Fig. 4A). We first determined that intra-VTA infusions of CNO in Cre^- controls did not produce changes in baseline DA release (Student's t test: $t_{(41)} = 1.163$, $p = 0.252$; Fig. 5A), uptake (Student's t test: $t_{(41)} = 0.035$, $p = 0.972$; Fig. 5B) nor cocaine potency relative to
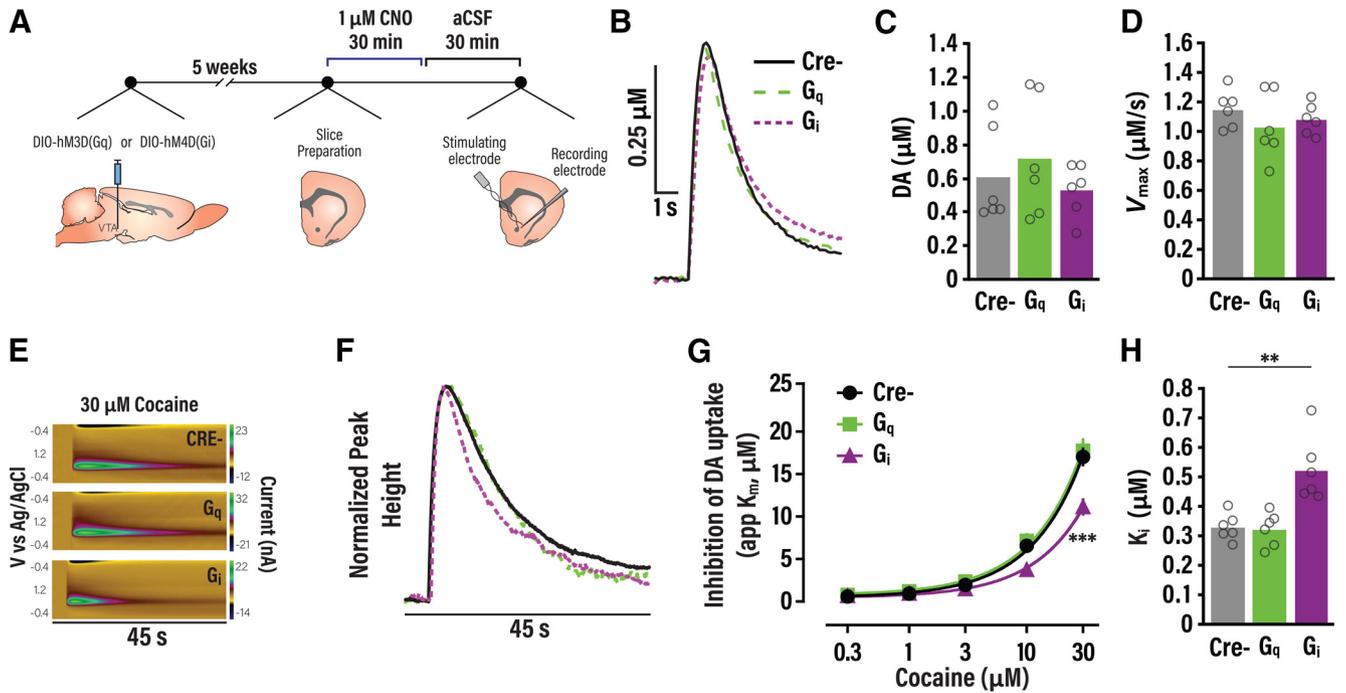
Figure 3. Activation of axonal G_i DREADDs reduces cocaine potency at proximal DATs. **A**, Experimental timeline. **B**, Example traces of stimulated DA release at baseline for Cre⁻, Cre⁺:G_q, and Cre⁺:G_i rats. **C**, Average DA release at baseline. **D**, Average DA uptake rate (V_{max}) at baseline. Example (**E**) color plots and (**F**) current versus time plots of DA release and uptake in the presence of cocaine (30 μM) for Cre⁻, Cre⁺:G_q, and Cre⁺:G_i rats. **G**, Inhibition of DA uptake following cumulative concentrations of cocaine (0.3-30 μM). **H**, Average cocaine K_i. Data are mean ± SEM. $n = 6$ for all groups. Dunnett's *post hoc*: ***$p < 0.001$; **$p < 0.01$ versus Cre⁻ control.
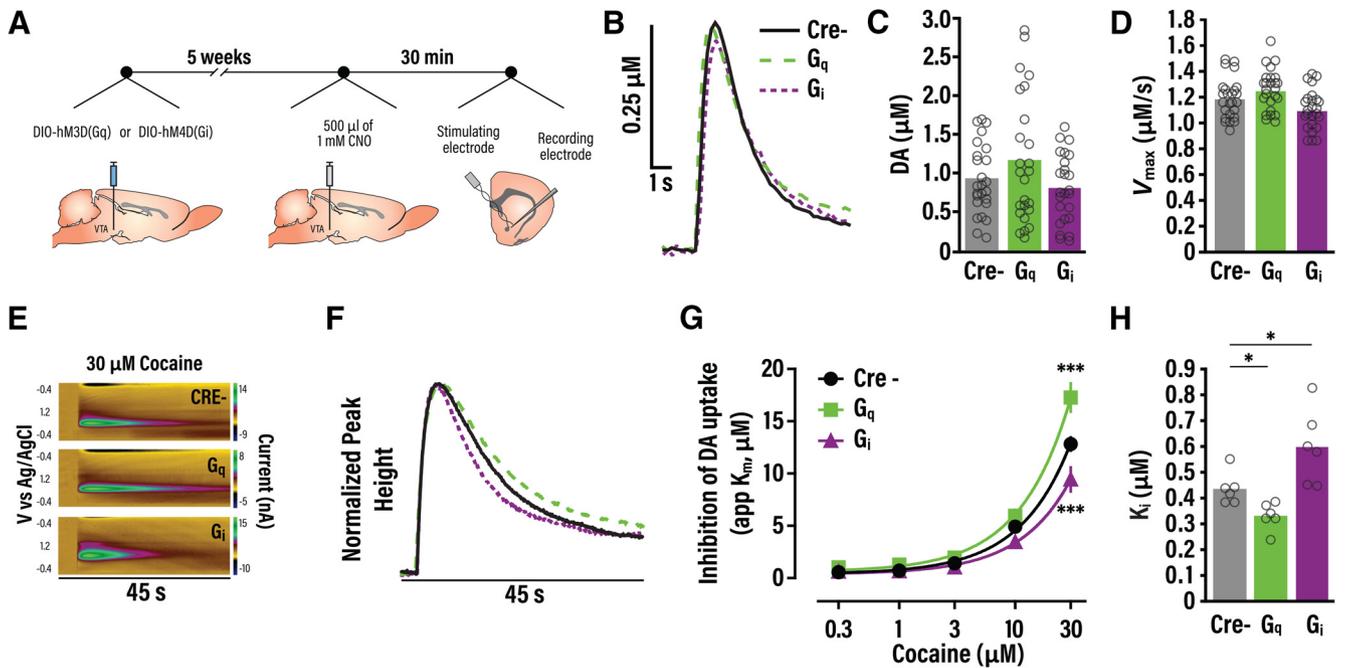
Figure 4. Activation of somatodendritic G_q and G_i DREADDs produces rapid, bidirectional changes in cocaine potency at distal DATs. **A**, Experimental timeline. **B**, Example traces of stimulated DA release at baseline for Cre⁻, Cre⁺:G_q, and Cre⁺:G_i rats. **C**, Average DA release at baseline. **D**, Average DA uptake rate (V_{max}) at baseline. **E**, Example color plots and current versus time plots of DA release and uptake in the presence of cocaine (30 μM) for Cre⁻, Cre⁺:G_q, and Cre⁺:G_i rats. **G**, Inhibition of DA uptake following cumulative cocaine concentrations (0.3-30 μM). **H**, Average cocaine K_i. Data are mean ± SEM. **C**, **D**, $n = 25$ per group; **G**, **H**, $n = 6$ per group. Dunnett's *post hoc*: ***$p < 0.001$; *$p < 0.05$ Cre⁻ control.

naive littermates (two-way ANOVA with group as the between-subjects measure and cocaine concentration as the repeated measure: Cocaine: $F_{(4,40)} = 157.0$, $p < 0.001$; group: $F_{(1,10)} = 0.469$, $p = 0.509$; Cocaine × group: $F_{(4,40)} = 0.664$, $p = 0.621$; Fig. 5C).

We then tested the effects of intra-VTA CNO infusions in Cre⁺:G_q or Cre⁺:G_i rats relative to Cre⁻ controls. Activation of G_q or G_i DREADDs did not have an effect on baseline DA release (one-way ANOVA: $F_{(2,15)} = 1.944$, $p = 0.151$; Fig. 4B,C) or
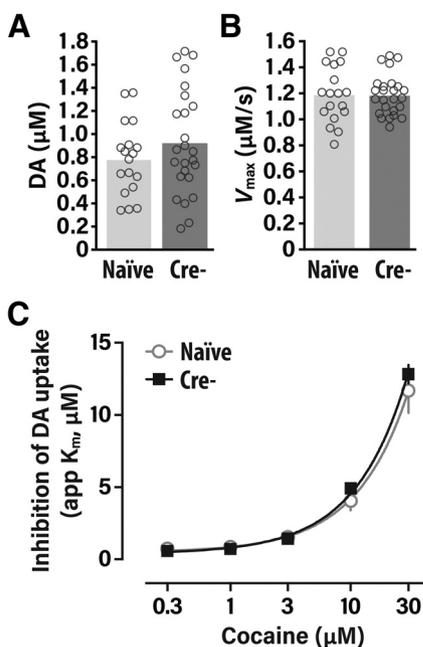
Figure 5. Intra-VTA microinfusion of CNO does not alter baseline DA release, uptake, or cocaine potency. **A**, Average DA release at baseline. **B**, Average DA uptake rate (V_{max}) at baseline. **C**, Inhibition of DA uptake following cumulative concentrations of cocaine (0.3-30 μM). Data are mean $\pm$ SEM. **A**, **B**, Naive, $n = 18$; Cre^-, $n = 25$. **C**, $n = 6$ per group.

uptake relative to Cre^- controls (one-way ANOVA: $F_{(2,15)} = 1.334$, $p = 0.269$; Fig. 4B,D). However, activation of G_q DREADDs increased cocaine potency, whereas activation of G_i DREADDs decreased cocaine potency (two-way ANOVA with DREADDs group as the between-subjects measure and cocaine concentration as the repeated measure: DREADDs: $F_{(2,15)} = 12.31$, $p < 0.001$; Cocaine $F_{(4,60)} = 378.1$, $p < 0.001$; DREADDs × Cocaine: $F_{(8,60)} = 11.11$, $p < 0.001$; Fig. 4E,G). These changes in cocaine potency corresponded with decreased cocaine K_i following activation of G_q DREADDs and increased cocaine K_i following activation of G_i DREADDs (one-way ANOVA: $F_{(2,15)} = 11.71$, $p < 0.001$; Fig. 4H). These observations demonstrate that selective activation of DREADDs in the somatodendritic compartment of DA neurons is sufficient to produce rapid, bidirectional changes in cocaine potency at distal DATs in the NAc. To further explore this phenomenon without potential confounds derived from activation of axonal DREADDs, all remaining experiments used intra-VTA microinfusions of CNO to exclusively activate DREADDs in the somatodendritic compartment of DA neurons.

Activation of somatodendritic G_q and G_i DREADDs on DA neurons alters cocaine potency through changes in the availability of the DAT cocaine binding site
We next tested whether activation of intra-VTA DREADDs drives generalized changes in the potency of DAT inhibitors. To this end, we tested whether activation of somatodendritic G_q and G_i DREADDs affects the potency of the noncanonical DAT inhibitor JHW 007. Cocaine preferentially binds and stabilizes the outward-open conformation of the DAT, whereas JHW 007 does not bind to the cocaine binding site and instead inhibits DA transport by stabilization of the inward-occluded DAT conformation (Robarge et al., 2000; Abramyan et al., 2017; Zou et al., 2017). Changes in JHW 007 potency would thus indicate that

differences in cocaine potency may be associated with general changes in DAT availability or function. We found that activation of G_q or G_i DREADDs had no effect on the ability of JHW 007 to inhibit DA uptake (two-way ANOVA with DREADDs group as the between-subjects measure and JHW 007 concentration as the repeated measure: JHW 007: $F_{(4,60)} = 83.49$, $p < 0.001$; DREADDs: $F_{(2,15)} = 0.005$, $p = 0.995$; DREADDs × JHW 007: $F_{(8,60)} = 0.250$, $p = 0.9789$; Fig. 6A–C). This lack of effect on JHW 007 potency suggests that changes in cocaine potency observed in our previous studies are not caused by gross changes in DAT availability or function.

We next examined whether activation of DREADDs changes the affinity of the DAT for cocaine through alterations in cocaine binding site dynamics. To test this, we used the high-affinity cocaine analog PTT. PTT is a tropane cocaine analog that is posited to bind to the DAT at the same binding site as cocaine and thus likely inhibits DA transport by stabilization of the outward facing DAT conformation (Davies et al., 1993; Bennett et al., 1995; Beuming et al., 2008). If activation of DREADDs on DA neuron soma influences the affinity of the DAT for cocaine through modifications in cocaine binding site dynamics, then activation of DREADDs should also alter PTT potency. We found that activation of G_q DREADDs increased PTT potency, whereas activation of G_i DREADDs decreased PTT potency (two-way ANOVA with DREADDs group as the between-subjects measure and PTT concentration as the repeated measure: DREADDs: $F_{(2,15)} = 10.65$, $p < 0.01$; PTT: $F_{(4,60)} = 281.4$, $p < 0.001$; DREADDs × PTT: $F_{(8,60)} = 6.251$, $p < 0.001$; Fig. 6D–F). The observation that activation of G_q and G_i DREADDs on DA neuron soma alters PTT potency in a similar manner as cocaine potency suggests that changes in cocaine potency may occur via modulation of cocaine binding dynamics.

Amine transporters, including the DAT, are posited to cycle through outward and inward facing conformations during normal transport (Forrest et al., 2008). It has been proposed that cocaine preferentially binds the outward facing conformation (Beuming et al., 2006); thus, one mechanism by which changes in cocaine affinity for the DAT may occur is through alterations in the stability of the outward facing DAT conformation. Previous work indicates that Zn^{2+} binds to the DAT and stabilizes the outward facing conformation (Norregaard et al., 1998; Loland et al., 1999). In line with this, Zn^{2+} increases binding of cocaine analogs (Moritz et al., 2013; Challasivakanaka et al., 2017) and increases the potency of cocaine and cocaine analogs (Loland et al., 2002, 2004). We found that 20 μM Zn^{2+} produced modest DA uptake inhibition on its own, but that the effect of Zn^{2+} on uptake inhibition produced by cocaine was significantly greater (paired Student's t test: $t_{(8)} = 3.852$, $p < 0.01$; Fig. 7). These observations indicate that Zn^{2+} and cocaine have a synergistic effect on DA uptake inhibition and, when considered with the existent literature, support the hypothesis that Zn^{2+} enhances cocaine potency by increasing availability of the cocaine binding site through stabilization of the outward facing DAT conformation (Norregaard et al., 1998; Loland et al., 1999, 2002, 2004; Moritz et al., 2013; Challasivakanaka et al., 2017).

We leveraged this characteristic of Zn^{2+} to test whether activation of G_q and G_i DREADDs on DA neuron soma modifies cocaine binding site dynamics by biasing the DAT toward the outward facing conformation. We hypothesized that activation of G_q DREADDs enhances cocaine potency by stabilizing the outward facing DAT conformation. Thus, we predicted that the effect of Zn^{2+} on cocaine potency would be blunted following activation of G_q DREADDs because G_q-mediated activation of
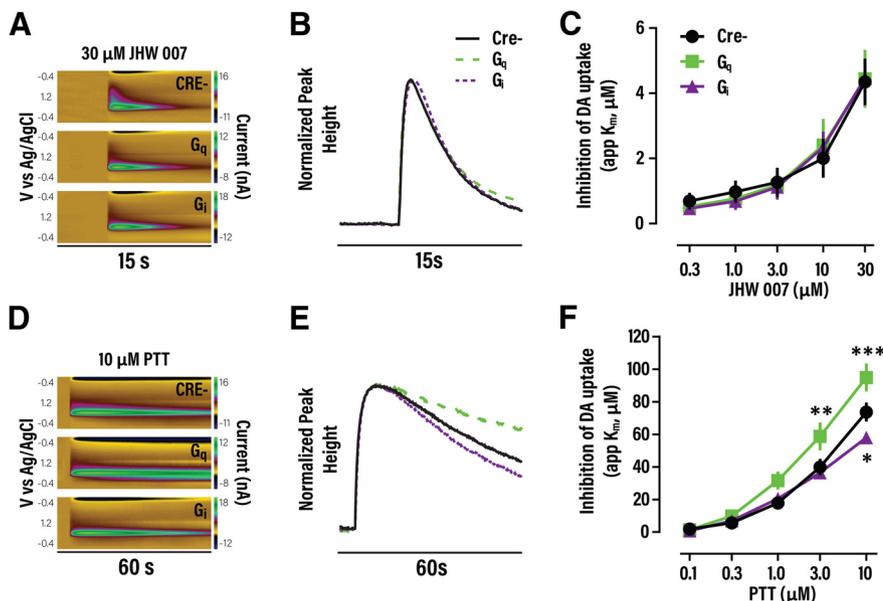
Figure 6. Activation of somatodendritic G_q and G_i DREADDs produces rapid, bidirectional changes in the stability of the cocaine binding site at distal DATs. Example (**A**) color plots and (**B**) current versus time plots of DA release and uptake in the presence of the noncanonical DAT inhibitor JHW 007 (30 μM) for Cre$^-$, Cre$^+$:G_q, and Cre$^+$:G_i rats. **C**, Inhibition of DA uptake following cumulative JHW 007 concentrations (0.3-30 μM). Example (**D**) color plots and (**E**) current versus time plots of stimulated DA release and uptake in the presence of the cocaine analog PTT (10 μM) for Cre$^-$, Cre$^+$:G_q, and Cre$^+$:G_i rats. **F**, Inhibition of DA uptake following cumulative PTT concentrations (0.1-10 μM). Data are mean $\pm$ SEM. $n = 6$ for all groups. Dunnett's *post hoc*: ***$p < 0.001$; **$p < 0.01$; *$p < 0.05$ versus Cre$^-$ control.

DA neurons and Zn^{2+} increase cocaine potency at the DAT through a common mechanism. Conversely, we hypothesized that activation of G_i DREADDs decreases cocaine potency by destabilization of the outward facing DAT conformation. Thus, we predicted that the effects of Zn^{2+} on cocaine potency would be enhanced following activation of G_i DREADDs. To test this, we first determined DA uptake inhibition produced by 30 μM cocaine in slices prepared from Cre$^-$ controls, as well as Cre$^+$:G_q or Cre$^+$:G_i rats that received intra-VTA microinfusions of CNO. We replicated our finding that somatodendritic activation of G_q or G_i DREADDs alters cocaine potency at the DAT (two-way ANOVA with DREADDs group as the between-subjects measure and Zn^{2+} condition as the repeated measure: DREADDs: $F_{(2,15)}$ = 73.90, $p < 0.001$; Zn^{2+}: $F_{(1,2)}$ = 73.90, $p < 0.01$; DREADDs $\times$ Zn^{2+}: $F_{(2,2)}$ = 18.33, $p < 0.001$; Fig. 8A,B). We then monitored DA uptake inhibition following the addition of 20 μM Zn^{2+} and found that Zn^{2+}-induced increases in cocaine potency were blunted following activation of G_q DREADDs and enhanced following activation of G_i DREADDs (one-way ANOVA: $F_{(2,17)}$ = 18.33, $p < 0.001$; Fig. 8B,C). This evidence supports the hypothesis that chemogenetic manipulations that signal through G_q rapidly bias distal DATs toward the outward facing conformation, whereas chemogenetic manipulations that signal through G_i produce the opposite effect.

Activation of somatodendritic G_q and G_i DREADDs on DA neurons alters Thr-53 DAT phosphorylation
The outward facing DAT conformation can be stabilized by phosphorylation at Thr-53, and the DAT undergoes some degree of constant tonic phosphorylation at this site (Challasivakanaka et al., 2017). Thus, one mechanism through which activation of G_q and G_i DREADDs on DA neurons may influence DAT transporter conformation is through DAT phosphorylation and dephosphorylation at the Thr-53 site. We tested whether activation of somatodendritic DREADDs alters membrane DAT levels or Thr-53 phosphorylation using Western blots (Fig. 9A). Neither activation of G_q or G_i DREADDs had any effect on membrane DAT levels (one-way ANOVA: $F_{(2,26)}$ = 0.771, $p = 0.47$; Fig. 9B, C). However, activation of G_q DREADDs increased membrane DAT Thr-53 phosphorylation, whereas activation of G_i DREADDs reduced membrane DAT Thr-53 phosphorylation (one-way ANOVA: $F_{(2,26)}$ = 12.83, $p < 0.001$ Fig. 9B,D). These findings are consistent with the hypothesis that chemogenetic manipulations drive rapid changes in DAT conformation bias and cocaine binding that are associated with changes in DAT Thr-53 phosphorylation.

Activation of somatodendritic G_q and G_i DREADDs on DA neurons determines cocaine consumption
Our FSCV observations indicate that activation of G_q and G_i DREADDs on DA neuron soma dictates cocaine potency at distal DATs. However, the relevance of these changes to cocaine-taking is unknown. Rats titrate blood levels of cocaine and accumbens DA levels tightly (Wise et al., 1995), and increasing the effective DA response to cocaine results in compensatory decreases in cocaine consumption, whereas reductions in the effective DA response to cocaine result in compensatory increases in cocaine consumption (De Wit and Wise, 1977; Barrett et al., 2004; Oleson et al., 2011; Mahler et al., 2019).

Previously, we found that systemic injections of CNO in TH: Cre rats expressing excitatory G_q, or inhibitory G_i-DREADDs in VTA DA neurons robustly altered both the preferred blood levels for cocaine self-administered at low effort, as well as the degree of motivation to maintain those blood levels (Mahler et al., 2019). However, this prior study did not differentiate between behavioral effects of CNO acting at somatodendritic DREADDs from those acting at axonally expressed DREADDs, both of which occur after systemic CNO in this preparation (Mahler et al., 2019).

Therefore, we compared the behavioral effects of systemic CNO with those of CNO applied directly to VTA DA soma (Fig. 10A). Similar to our previous study (Mahler et al., 2019), we found that systemic activation of G_q DREADDs reduced low effort cocaine consumption (Q_o), whereas activation of G_i DREADDs increased Q_o (two-way ANOVA with DREADDs group as the between-subjects measure and CNO treatment as the repeated measure: DREADDs: $F_{(2,15)}$ = 12.64, $p < 0.001$; CNO $F_{(1,15)}$ = 0.001, $p = 0.981$; DREADDs $\times$ CNO: $F_{(2,15)}$ = 10.64, $p < 0.01$; Fig. 10B). Similar effects on Q_o were observed after intra-VTA activation of G_q or G_i DREADDs (two-way ANOVA with DREADDs group as the between-subjects measure and CNO treatment as the repeated measure: DREADDs: $F_{(2,15)}$ = 4.374, $p < 0.05$; CNO: $F_{(1,15)}$ = 0.001, $p = 0.990$, DREADDs $\times$ CNO: $F_{(2,15)}$ = 8.425, $p < 0.01$; Fig. 10C). As expected, no effects of either systemic or intra-VTA CNO were observed in Cre$^-$ control
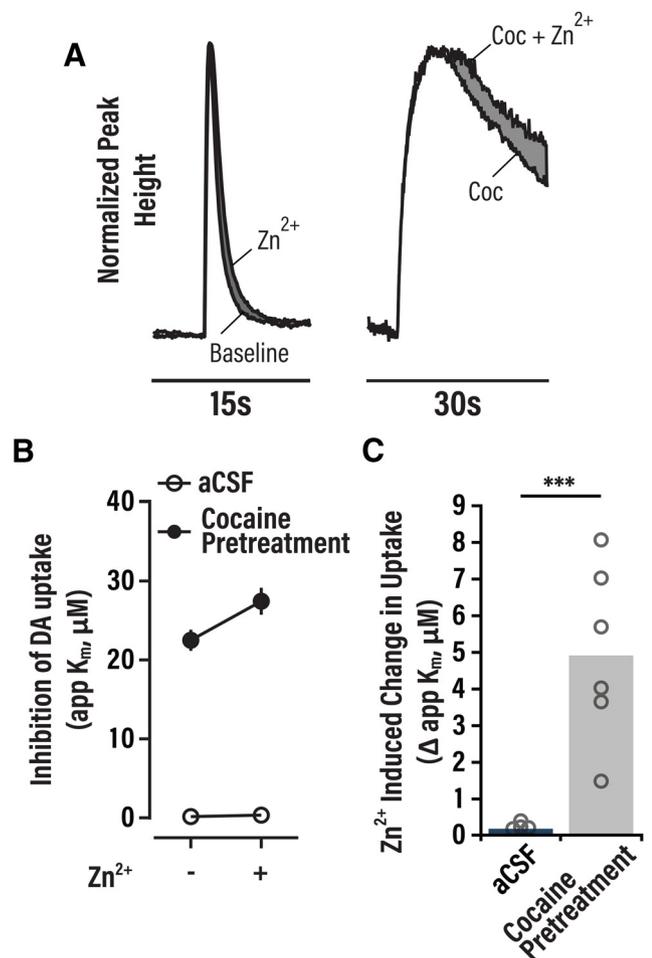
Figure 7. Zn^{2+} enhances cocaine-induced inhibition of DA uptake. **A**, Example current versus time plots at baseline, after the addition of Zn^{2+}, in the presence of 30 μM cocaine, and in the presence of 30 μM cocaine with 20 μM Zn^{2+}. Shaded regions represent the enhanced inhibition of DA uptake following the addition of Zn^{2+}. **B**, Inhibition of DA uptake before and after the addition of Zn^{2+} (20 μM) to brain slices preincubated with aCSF or with cocaine (30 μM). **C**, Change in DA uptake produced by the addition of Zn^{2+} (20 μM). Data are mean $\pm$ SEM. $n = 4$ aCSF, $n = 6$ cocaine pretreatment. ***$p < 0.001$ versus aCSF control.

rats. These observations are in line with our pharmacological data as increases in cocaine potency observed following activation of G_q DREADDs produced compensatory decreases in cocaine consumption, whereas reductions in cocaine potency observed following activation of G_i DREADDs produced compensatory increases in cocaine consumption.

Consistent with our previous work (Mahler et al., 2019), systemic activation of DREADDs also influenced motivation for cocaine. We found that activation of G_q DREADDs decreased cocaine demand elasticity, which represents an increase in motivation for cocaine, whereas activation of G_i DREADDs increased cocaine demand elasticity, which represents a reduction in motivation for cocaine (two-way ANOVA with DREADDs group as the between-subjects measure and CNO treatment as the repeated measure: DREADDs: $F_{(2,15)} = 11.12$, $p < 0.01$; CNO: $F_{(1,15)} = 0.112$, $p = 0.743$; DREADDs × CNO: $F_{(2,15)} = 90.02$, $p < 0.001$; Fig. 10D). However, intra-VTA activation of either G_q or G_i DREADDs had no effect on motivation for cocaine (two-way ANOVA with DREADDs group as the between-subjects measure and CNO treatment as the repeated measure: DREADDs: $F_{(2,15)} = 0.453$, $p = 0.644$; CNO $F_{(1,15)} = 1.058$,
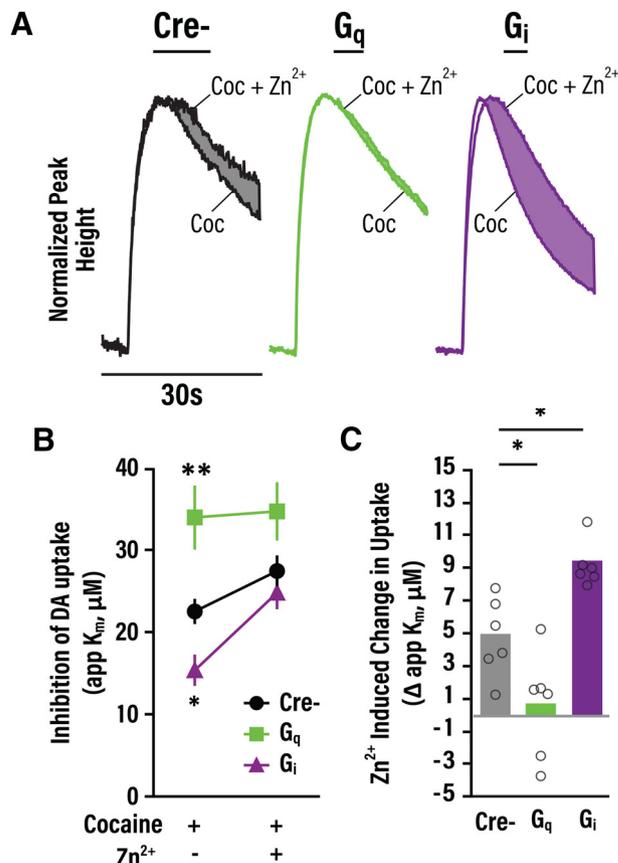
Figure 8. Activation of somatodendritic G_q and G_i DREADDs produces rapid, bidirectional changes in the stability of the outward facing DAT conformation. **A**, Example current versus time plots in the presence of 30 μM cocaine and 30 μM cocaine with 20 μM Zn^{2+} for Cre⁻, Cre⁺:G_q, and Cre⁺:G_i rats. Shaded regions represent inhibition of DA uptake following the addition of Zn^{2+}. **B**, Inhibition of DA uptake before and after the addition of Zn^{2+} (20 μM) to brain slices bathed in cocaine (30 μM). **C**, Change in inhibition of DA uptake following addition of Zn^{2+} (20 μM) to brain slices bathed in cocaine (30 μM). Data are mean $\pm$ SEM. $n = 6$ for all groups. Dunnett's *post hoc*: **$p < 0.01$; *$p < 0.05$ versus Cre⁻ control.

$p = 0.320$; DREADDs × CNO; $F_{(2,15)} = 0.1376$, $p = 0.873$; Fig. 10E). This difference between systemic and intra-VTA activation of DREADDs suggests that modulation of neurotransmitter release by axonally expressed DREADDs plays a crucial role in effortful cocaine seeking, consistent with the proseeking effects of direct axonal manipulations that we have previously reported (Mahler et al., 2019). Future experiments parsing the effects of GPCR activation in the axonal versus somatodendritic compartments will be critical to uncovering the complexity of mesolimbic DA circuits in driving drug-associated behavior.

Discussion

The current studies demonstrate that GPCRs on DA neurons exert rapid and bidirectional control over cocaine potency at distal DATs. We showed that activation of excitatory or inhibitory DREADDs on DA neuron soma produced rapid, bidirectional changes in cocaine potency at distal DATs in the NAc, as well as concordant alterations in cocaine consumption. We further demonstrate that changes in cocaine potency at distal DATs are likely to occur through rapid alterations in DAT phosphorylation and conformation biases that influence the affinity of cocaine for the DAT. Together, these studies provide a novel mechanism whereby GPCRs modulate pharmacodynamic properties of cocaine that influence cocaine-associated behavior.
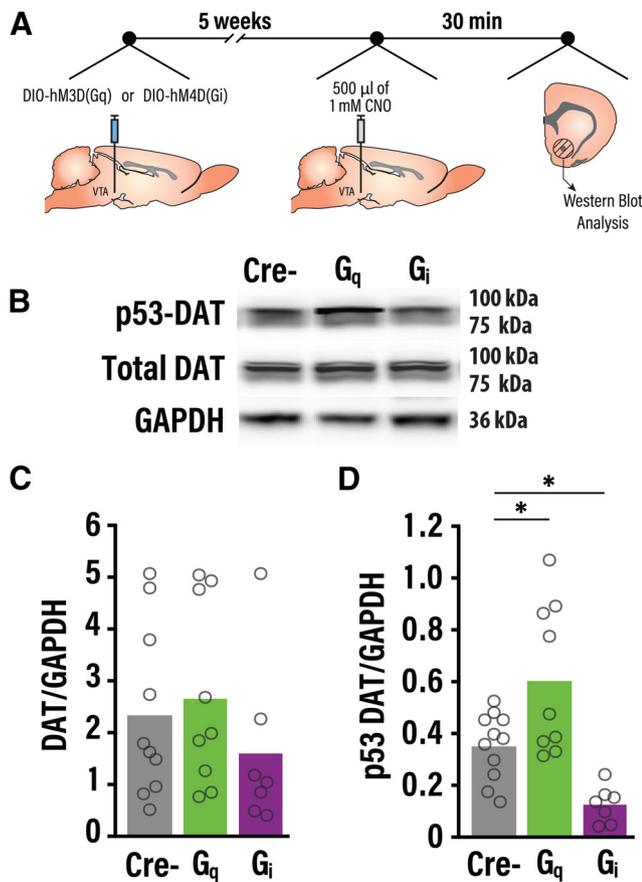
Figure 9. Activation of somatodendritic G_q and G_i DREADDs produces rapid, bidirectional changes in DAT phosphorylation at Thr-53. *A*, Experimental timeline. *B*, Western blot analysis for total DAT protein and Thr-53 phosphorylated DAT in the membrane fraction. *C*, Total DAT levels for Cre^-, Cre^+:G_q, and Cre^+:G_i rats. *D*, Thr-53 phosphorylated DAT for Cre^-, Cre^+:G_q, and Cre^+:G_i rats. Data are mean. Cre^-, $n = 11$; G_q, $n = 9$; G_i, $n = 7$. *$p < 0.05$ (Dunnett's *post hoc*).

Figure 10. Activation of somatodendritic G_q and G_i DREADDs produces rapid, bidirectional changes in cocaine consumption. *A*, Experimental timeline. *B*, Systemic CNO effects on cocaine consumption. *C*, Intra-VTA CNO effects on cocaine consumption. *D*, Systemic CNO effects on motivation for cocaine. *E*, Intra-VTA CNO effects on motivation for cocaine. Data are mean. Cre^-, $n = 6$; G_q, $n = 8$; G_i, $n = 5$ or 6. Fisher's LSD test was used *post hoc* to determine significant effects of CNO relative to vehicle: ***$p < 0.001$; **$p < 0.01$; *$p < 0.05$.

Mechanisms underlying somatodendritic GPCR effects on cocaine potency at distal DATs

Activation of GPCRs is known to influence the function of proximal DATs by the direct action of effector molecules that result from the activation of traditional signaling cascades (Schmitt and Reith, 2010; Bermingham and Blakely, 2016; Foster and Vaughan, 2017). Indeed, we found that incubation of NAc slices where G_i DREADDs in DA axons are proximal to DATs resulted in a reduction in cocaine potency, which is consistent with prior work showing robust effects of G_i-coupled GPCR signaling on proximal DATs (Karkhanis et al., 2017; Fagan et al., 2020). However, live imaging studies have shown that activation of GPCRs produce compartmentalized effects such that changes in effector molecule concentrations operate along a spatial gradient that extends no farther than 20–25 µm from the site of GPCR activation (Kholodenko, 2006; Calebiro and Koszegi, 2019; Halls, 2019). Further, such effector molecule concentrations are poorly transmitted through axons where effector molecule gradients extend no farther than 15 µm (Maiellaro et al., 2016). In our studies, the distance between the neuron soma and DATs in the NAc is ~7200 µm (Swanson, 1998); thus, it is unlikely that the recruitment of traditional signaling cascades and resulting changes in effector molecule concentrations could directly influence DATs in the NAc following intra-VTA manipulations.

Activation of somatodendritic GPCRs may also produce changes in gene transcription and translation (Musnier et al., 2010), and such changes may ultimately influence DAT function. In the current studies, we mitigate the potential for such effects by temporal constraints. For changes in transcription or translational to influence distal DATs in the NAc, protein products would need to be physically translocated along the axon from DA neuron soma to release sites where they may interact with DATs. The fastest known means by which a protein may be transported through an axon is fast axonal transport. Fast axonal transport proceeds at 35–139 µm/min (Hill et al., 2004; Roy, 2014); thus, at least ~52 min would be required to transport proteins the ~7200 µm from DA neuron soma to DATs in the NAc. In the current studies, we allowed 30 min between intra-VTA administration of CNO and NAc brain slice preparation in which DA axons are severed. Thus, our experiments do not allow sufficient time for fast axonal transport to move gene products from DA neuron soma in the VTA to DATs in the NAc. Therefore, it is unlikely that GPCR-mediated changes in transcription/translation are a major factor in the cocaine potency alterations observed in the current work.

Activation of GPCRs on DA neurons rapidly alters DA neuron resting membrane potential, excitability, firing rate, and

firing pattern (Korotkova et al., 2003, 2006; Margolis et al., 2003; Ungless et al., 2003; Borgland et al., 2006, 2009; Muschamp et al., 2007, 2014; Moorman and Aston-Jones, 2010; Werkman et al., 2011; Baimel et al., 2017; Runegaard et al., 2018; Fitzpatrick et al., 2019; Mahler et al., 2019), and these changes in the electrical properties of neurons are rapidly transmitted along the axon. Previous work indicates that the functional state of DATs is directly influenced by electrical changes *in vitro* (Woodward et al., 1986; Sonders et al., 1997; Richardson et al., 2016), and the concept that GPCR modulation of DA neuron activity may influence cocaine potency at distal DATs has been put forward previously. Indeed, hypocretin-induced elevations in DA neuron firing rate (Moorman and Aston-Jones, 2010) correspond with elevations in NAc cocaine potency (España et al., 2011; Brodnik et al., 2020). Likewise, elevations in circulating estradiol levels correlate with increases in DA neuron firing and NAc cocaine potency (Calipari et al., 2017). Furthermore, it has been shown that two daily systemic activations of G_q DREADDs on DA neurons increase NAc cocaine potency (Calipari et al., 2017), similar to our initial findings using acute systemic activation of G_q DREADDs. Unlike our current experiments, however, changes in cocaine potency observed following repeated systemic CNO could be associated with direct CNO effects on axonal DREADDs and/or changes in gene transcription or translation.

The current studies were explicitly designed to mitigate the influence of terminal GPCR activity, the effects of traditional GPCR signaling cascades, and gene transcription and translation through spatial and temporal constraints. Thus, we posit that changes in DA neuron activity are the mostly likely cause of changes in cocaine potency at distal DATs. It remains unclear which specific changes in DA neuron activity may drive alterations in DAT cocaine sensitivity. Future work will need to use more direct experimental manipulations of DA neuron activity, such as optogenetics, to test whether *in vivo* DAT cocaine sensitivity is altered by discrete DA neuron activity changes, including membrane potential, DA neuron firing rate, or alterations in DA neuron firing patterns that include the frequency or duration of phasic burst firing events.

Intraterminal mechanisms for cocaine potency alterations at distal DATs

Cocaine potency is partially determined by the relative affinity of cocaine for its binding site on DATs, and cocaine potency is affected by DAT phosphorylation (Foster et al., 2012; Moritz et al., 2013; Challasivakanaka et al., 2017), oligomerization (Chen and Reith, 2007; Siciliano et al., 2018), and heteromerization (Hong et al., 2017). Such factors are readily influenced by the activity of intra-axonal kinases, which are posited to respond to changes in neuron activity (Moron et al., 2003; Gorentla et al., 2009; Schmitt and Reith, 2010; Foster et al., 2012; Bermingham and Blakely, 2016; Richardson et al., 2016; Foster and Vaughan, 2017). We found that alterations in cocaine potency corresponded with changes in DAT Thr-53 phosphorylation, suggesting that one intra-axonal mechanism for alterations in cocaine potency may involve phosphorylation of DATs.

The kinase for Thr-53 phosphorylation remains unknown; however, proline-directed motifs, such as the DAT Thr-53 site, are bound by only a few kinases. Mitogen-activated protein kinase (Ubersax and Ferrell, 2007) is one candidate kinase for Thr-53 phosphorylation, and recent work suggests that indices of mitogen-activated protein kinase signaling, DAT phosphorylation, and cocaine potency are all elevated under conditions of

increased DA neuron firing (Calipari et al., 2017). Alternatively, changes in membrane potential drive direct interactions between CaMKIIα and membrane DATs (Richardson et al., 2016); thus, CaMKIIα may also participate in alterations in DAT function. Additional work will need to define the signaling pathways through which DA neuron activity influences DAT phosphorylation and cocaine potency.

GPCR-induced changes in DA neuron activity alter cocaine consumption

In line with the observed changes in cocaine potency, we found that intra-VTA activation of DA neuron DREADDs produced bidirectional changes in cocaine consumption. This observation matches previous work demonstrating that systemic activation of G_q DREADDs enhanced cocaine CPP (Calipari et al., 2017) and decreased preferred self-administered cocaine dose (Mahler et al., 2019). Similarly, systemic activation of G_i DREADDs suppressed locomotor response to cocaine (Runegaard et al., 2018), and increased preferred self-administered cocaine dose (Mahler et al., 2019). Here we found that intra-VTA G_q DREADD activation decreased cocaine consumption, whereas intra-VTA activation of G_i DREADDs increased cocaine consumption. Overall, these observations support the hypothesis that GPCRs on DA neurons play a pivotal role in determining cocaine consumption via modulation of cocaine potency at distal DATs.

We also found that systemic activation of DA neuron DREADDs produced bidirectional changes in motivation for cocaine that were not observed when rats received intra-VTA activation of DREADDs. These findings suggest that systemic activation of DREADDs on DA neurons recruits processes critical for determining motivation for cocaine, whereas activation of somatodendritic DREADDs alone does not. While studies using DA neuron ablation or nonspecific pharmacological inactivation of DA neurons have established that DA neuron firing is required for cocaine self-administration (Roberts et al., 1977; Caine and Koob, 1994; Brebner et al., 2000; Di Ciano and Everitt, 2004), our data demonstrate that bidirectional activation of DREADDs produces specific effects on cocaine consumption but does not directly influence motivation for cocaine. It has recently been discovered that NAc DA signals associated with motivation occur independently from DA neuron activity, and thus are likely generated through local NAc microcircuitry (Mohebi et al., 2019). It is therefore possible that intra-VTA DREADDs manipulations do not influence motivation for cocaine because motivation-associated DA signals are not generated through changes in VTA DA neuron activity.

In conclusion, the current findings outline a process by which GPCR modulation of DA neuron activity governs cocaine potency at the DAT via phosphorylation at Thr-53 and subsequent stabilization of the outward facing DAT conformation. Many endogenous GPCRs expressed on DA neurons have been described as important in the pathology of cocaine use disorder or have been identified as potential therapeutic targets for the treatment of cocaine use disorder. Furthermore, DA neuron activity varies across psychiatric disorders (Marinelli and McCutcheon, 2014; Pignatelli and Bonci, 2015; Salamone et al., 2015; Grace, 2016), and is subject to plastic changes following a wide spectrum of insults, including stress (Tye et al., 2013; Friedman et al., 2014), exposure to pharmacological agents (Juarez and Han, 2016; Kokkinou et al., 2018), and drug abuse history (Stuber et al.,

2010; Volkow et al., 2017). Our findings offer insight into the spectrum of ways in which cocaine use may vary as a result of altered DA neuron activity in these conditions (Brooner et al., 1997; Jacobsen et al., 2001; Roncero et al., 2012). Thus, this work has additional implications for understanding the regulation of cocaine consumption across stages of addiction, and for the mechanisms that underlie a variety of cocaine use disorder comorbidities.

References

Abramyan AM, Stolzenberg S, Li Z, Loland CJ, Noe F, Shi L (2017) The isomeric preference of an atypical dopamine transporter inhibitor contributes to its selection of the transporter conformation. ACS Chem Neurosci 8:1735–1746.

Baimel C, Lau BK, Qiao M, Borgland SL (2017) Projection-target-defined effects of orexin and dynorphin on VTA dopamine neurons. Cell Rep 18:1346–1355.

Barrett AC, Miller JR, Dohrmann JM, Caine SB (2004) Effects of dopamine indirect agonists and selective D1-like and D2-like agonists and antagonists on cocaine self-administration and food maintained responding in rats. Neuropharmacology 47:256–273.

Bennett BA, Wichems CH, Hollingsworth CK, Davies HM, Thornley C, Sexton T, Childers SR (1995) Novel 2-substituted cocaine analogs: uptake and ligand binding studies at dopamine, serotonin and norepinephrine transport sites in the rat brain. J Pharmacol Exp Ther 272:1176–1186.

Bentzley BS, Fender KM, Aston-Jones G (2013) The behavioral economics of drug self-administration: a review and new analytical approach for within-session procedures. Psychopharmacology 226:113–125.

Berke JD, Hyman SE (2000) Addiction, dopamine, and the molecular mechanisms of memory. Neuron 25:515–532.

Bermingham DP, Blakely RD (2016) Kinase-dependent regulation of monoamine neurotransmitter transporters. Pharmacol Rev 68:888–953.

Beuming T, Shi L, Javitch JA, Weinstein H (2006) A comprehensive structure-based alignment of prokaryotic and eukaryotic neurotransmitter/Na$^+$ symporters (NSS) aids in the use of the LeuT structure to probe NSS structure and function. Mol Pharmacol 70:1630–1642.

Beuming T, Kniazeff J, Bergmann ML, Shi L, Gracia L, Raniszewska K, Newman AH, Javitch JA, Weinstein H, Gether U, Loland CJ (2008) The binding sites for cocaine and dopamine in the dopamine transporter overlap. Nat Neurosci 11:780–789.

Borgland SL, Taha SA, Sarti F, Fields HL, Bonci A (2006) Orexin A in the VTA is critical for the induction of synaptic plasticity and behavioral sensitization to cocaine. Neuron 49:589–601.

Borgland SL, Chang SJ, Bowers MS, Thompson JL, Vittoz N, Floresco SB, Chou J, Chen BT, Bonci A (2009) Orexin A/hypocretin-1 selectively promotes motivation for positive reinforcers. J Neurosci 29:11215–11225.

Brebner K, Phelan R, Roberts DC (2000) Intra-VTA baclofen attenuates cocaine self-administration on a progressive ratio schedule of reinforcement. Pharmacol Biochem Behav 66:857–862.

Brodnik ZD, España RA (2015) Dopamine uptake dynamics are preserved under isoflurane anesthesia. Neurosci Lett 606:129–134.

Brodnik ZD, Ferris MJ, Jones SR, España RA (2017a) Reinforcing doses of intravenous cocaine produce only modest dopamine uptake inhibition. ACS Chem Neurosci 8:281–289.

Brodnik ZD, Black EM, Clark MJ, Kornsey KN, Snyder NW, España RA (2017b) Susceptibility to traumatic stress sensitizes the dopaminergic response to cocaine and increases motivation for cocaine. Neuropharmacology 125:295–307.

Brodnik ZD, Alonso IP, Xu W, Zhang Y, Kortagere S, España RA (2020) Hypocretin receptor 1 involvement in cocaine-associated behavior: therapeutic potential and novel mechanistic insights. Brain Res 1731:145894.

Brooner RK, King VL, Kidorf M, Schmidt CW, Bigelow GE (1997) Psychiatric and substance use comorbidity among treatment-seeking opioid abusers. Arch Gen Psychiatry 54:71–80.

Caine SB, Koob GF (1994) Effects of mesolimbic dopamine depletion on responding maintained by cocaine and food. J Exp Anal Behav 61:213–221.

Calebiro D, Koszegi Z (2019) The subcellular dynamics of GPCR signaling. Mol Cell Endocrinol 483:24–30.

Calipari ES, Ferris MJ, Jones SR (2014) Extended access of cocaine self-administration results in tolerance to the dopamine-elevating and locomotor-stimulating effects of cocaine. J Neurochem 128:224–232.

Calipari ES, Siciliano CA, Zimmer BA, Jones SR (2015) Brief intermittent cocaine self-administration and abstinence sensitizes cocaine effects on the dopamine transporter and increases drug seeking. Neuropsychopharmacology 40:728–735.

Calipari ES, Ferris MJ, Zimmer BA, Roberts DC, Jones SR (2013) Temporal pattern of cocaine intake determines tolerance vs sensitization of cocaine effects at the dopamine transporter. Neuropsychopharmacology 38:2385–2392.

Calipari ES, Juarez B, Morel C, Walker DM, Cahill ME, Ribeiro E, Roman-Ortiz C, Ramakrishnan C, Deisseroth K, Han MH, Nestler EJ (2017) Dopaminergic dynamics underlying sex-specific cocaine reward. Nat Commun 8:13877.

Challasivakanaka S, Zhen J, Smith ME, Reith ME, Foster JD, Vaughan RA (2017) Dopamine transporter phosphorylation site threonine 53 is stimulated by amphetamines and regulates dopamine transport, efflux, and cocaine analog binding. J Biol Chem 292:19066–19075.

Cheer JF, Wassum KM, Sombers LA, Heien ML, Ariansen JL, Aragona BJ, Phillips PE, Wightman RM (2007) Phasic dopamine release evoked by abused substances requires cannabinoid receptor activation. J Neurosci 27:791–795.

Chen N, Reith ME (2007) Substrates and inhibitors display different sensitivity to expression level of the dopamine transporter in heterologously expressing cells. J Neurochem 101:377–388.

Chen R, Tilley MR, Wei H, Zhou F, Zhou FM, Ching S, Quan N, Stephens RL, Hill ER, Nottoli T, Han DD, Gu HH (2006) Abolished cocaine reward in mice with a cocaine-insensitive dopamine transporter. Proc Natl Acad Sci USA 103:9333–9338.

Davies HM, Saikali E, Sexton T, Childers SR (1993) Novel 2-substituted cocaine analogs: binding properties at dopamine transport sites in rat striatum. Eur J Pharmacol 244:93–97.

De Wit H, Wise RA (1977) Blockade of cocaine reinforcement in rats with the dopamine receptor blocker pimozide, but not with the noradrenergic blockers phentolamine or phenoxybenzamine. Can J Psychol 31:195–203.

Desai RI, Kopajtic TA, Koffarnus M, Newman AH, Katz JL (2005) Identification of a dopamine transporter ligand that blocks the stimulant effects of cocaine. J Neurosci 25:1889–1893.

Di Ciano P, Everitt BJ (2004) Contribution of the ventral tegmental area to cocaine-seeking maintained by a drug-paired conditioned stimulus in rats. Eur J Neurosci 19:1661–1667.

Dunah AW, Standaert DG (2001) Dopamine D1 receptor-dependent trafficking of striatal NMDA glutamate receptors to the postsynaptic membrane. J Neurosci 21:5546–5558.

España RA, Oleson EB, Locke JL, Brookshire BR, Roberts DC, Jones SR (2010) The hypocretin-orexin system regulates cocaine self-administration via actions on the mesolimbic dopamine system. Eur J Neurosci 31:336–348.

España RA, Melchior JR, Roberts DC, Jones SR (2011) Hypocretin 1/orexin A in the ventral tegmental area enhances dopamine responses to cocaine and promotes cocaine self-administration. Psychopharmacology: 214:415–412.

Fagan RR, Kearney PJ, Melikian HE (2020) In situ regulated dopamine transporter trafficking: there's no place like home. Neurochem Res 45:1335–1343.

Ferris MJ, Calipari ES, Mateo Y, Melchior JR, Roberts DC, Jones SR (2012) Cocaine self-administration produces pharmacodynamic tolerance: differential effects on the potency of dopamine transporter blockers, releasers, and methylphenidate. Neuropsychopharmacology 37:1708–1716.

Fitzpatrick CM, Runegaard AH, Christiansen SH, Hansen NW, Jørgensen SH, McGirr JC, de Diego Ajenjo A, Sørensen AT, Perrier JF, Petersen A, Gether U, Woldbye DP, Andreasen JT (2019) Differential effects of chemogenetic inhibition of dopamine and norepinephrine neurons in the mouse 5-choice serial reaction time task. Prog Neuropsychopharmacol Biol Psychiatry 90:264–276.

Forrest LR, Zhang YW, Jacobs MT, Gesmonde J, Xie L, Honig BH, Rudnick G (2008) Mechanism for alternating access in neurotransmitter transporters. Proc Natl Acad Sci USA 105:10338–10343.

Foster JD, Vaughan RA (2011) Palmitoylation controls dopamine transporter kinetics, degradation, and protein kinase C-dependent regulation. J Biol Chem 286:5175–5186.

Foster JD, Vaughan RA (2017) Phosphorylation mechanisms in dopamine transporter regulation. J Chem Neuroanat 83-84:10–18.

Foster JD, Yang JW, Moritz AE, Challasivakanaka S, Smith MA, Holy M, Wilebski K, Sitte HH, Vaughan RA (2012) Dopamine transporter phosphorylation site threonine 53 regulates substrate reuptake and amphetamine-stimulated efflux. J Biol Chem 287:29702–29712.

Friedman AK, Walsh JJ, Juarez B, Ku SM, Chaudhury D, Wang J, Li X, Dietz DM, Pan N, Vialou VF, Neve RL, Yue Z, Han MH (2014) Enhancing depression mechanisms in midbrain dopamine neurons achieves homeostatic resilience. Science 344:313–319.

Gorentla BK, Moritz AE, Foster JD, Vaughan RA (2009) Proline-directed phosphorylation of the dopamine transporter N-terminal domain. Biochemistry 48:1067–1076.

Grace AA (2016) Dysregulation of the dopamine system in the pathophysiology of schizophrenia and depression. Nat Rev Neurosci 17:524–532.

Halls ML (2019) Localised GPCR signalling as revealed by FRET biosensors. Curr Opin Cell Biol 57:48–56.

Hill DB, Plaza MJ, Bonin K, Holzwarth G (2004) Fast vesicle transport in PC12 neurites: velocities and forces. Eur Biophys J 33:623–632.

Hong WC, Yano H, Hiranita T, Chin FT, McCurdy CR, Su TP, Amara SG, Katz JL (2017) The sigma-1 receptor modulates dopamine transporter conformation and cocaine binding and may thereby potentiate cocaine self-administration in rats. J Biol Chem 292:11250–11261.

Hurd YL, Ungerstedt U (1989) Cocaine: an in vivo microdialysis evaluation of its acute action on dopamine transmission in rat striatum. Synapse 3:48–54.

Hursh SR (1993) Behavioral economics of drug self-administration: an introduction. Drug Alcohol Depend 33:165–172.

Jacobsen LK, Southwick SM, Kosten TR (2001) Substance use disorders in patients with posttraumatic stress disorder: a review of the literature. Am J Psychiatry 158:1184–1190.

John CE, Jones SR (2007) Voltammetric characterization of the effect of monoamine uptake inhibitors and releasers on dopamine and serotonin uptake in mouse caudate-putamen and substantia nigra slices. Neuropharmacology 52:1596–1605.

Juarez B, Han MH (2016) Diversity of dopaminergic neural circuits in response to drug exposure. Neuropsychopharmacology 41:2424–2446.

Kalivas PW, O'Brien C (2008) Drug addiction as a pathology of staged neuroplasticity. Neuropsychopharmacology 33:166–180.

Karkhanis A, Holleran KM, Jones SR (2017) Dynorphin/kappa opioid receptor signaling in preclinical models of alcohol, drug, and food addiction. Int Rev Neurobiol 136:53–88.

Kholodenko BN (2006) Cell-signalling dynamics in time and space. Nat Rev Mol Cell Biol 7:165–176.

Kohtz AS, Lin B, Smith ME, Aston-Jones G (2018) Attenuated cocaine-seeking after oxytocin administration in male and female rats. Psychopharmacology 235:2051–2063.

Kokkinou M, Ashok AH, Howes OD (2018) The effects of ketamine on dopaminergic function: meta-analysis and review of the implications for neuropsychiatric disorders. Mol Psychiatry 23:59–69.

Korotkova TM, Sergeeva OA, Eriksson KS, Haas HL, Brown RE (2003) Excitation of ventral tegmental area dopaminergic and nondopaminergic neurons by orexins/hypocretins. J Neurosci 23:7–11.

Korotkova TM, Brown RE, Sergeeva OA, Ponomarenko AA, Haas HL (2006) Effects of arousal- and feeding-related neuropeptides on dopaminergic and GABAergic neurons in the ventral tegmental area of the rat. Eur J Neurosci 23:2677–2685.

Kuhar MJ, Ritz MC, Boja JW (1991) The dopamine hypothesis of the reinforcing properties of cocaine. Trends Neurosci 14:299–302.

Loland CJ, Norregaard L, Gether U (1999) Defining proximity relationships in the tertiary structure of the dopamine transporter: identification of a conserved glutamic acid as a third coordinate in the endogenous Zn (2+)-binding site. J Biol Chem 274:36928–36934.

Loland CJ, Norregaard L, Litman T, Gether U (2002) Generation of an activating Zn(2+) switch in the dopamine transporter: mutation of an intracellular tyrosine constitutively alters the conformational equilibrium of the transport cycle. Proc Natl Acad Sci USA 99:1683–1688.

Loland CJ, Granas C, Javitch JA, Gether U (2004) Identification of intracellular residues in the dopamine transporter critical for regulation of transporter conformation and cocaine binding. J Biol Chem 279:3228–3238.

Mahler SV, Brodnik ZD, Cox BM, Buchta WC, Bentzley BS, Quintanilla J, Cope ZA, Lin EC, Riedy MD, Scofield MD, Messinger J, Ruiz CM, Riegel

AC, España RA, Aston-Jones G (2019) Chemogenetic manipulations of ventral tegmental area dopamine neurons reveal multifaceted roles in cocaine abuse. J Neurosci 39:503–518.

Maiellaro I, Lohse MJ, Kittel RJ, Calebiro D (2016) cAMP signals in Drosophila motor neurons are confined to single synaptic boutons. Cell Rep 17:1238–1246.

Margolis EB, Hjelmstad GO, Bonci A, Fields HL (2003) Kappa-opioid agonists directly inhibit midbrain dopaminergic neurons. J Neurosci 23:9981–9986.

Marinelli M, McCutcheon JE (2014) Heterogeneity of dopamine neuron activity across traits and states. Neuroscience 282:176–197.

Mohebi A, Pettibone JR, Hamid AA, Wong JT, Vinson LT, Patriarchi T, Tian L, Kennedy RT, Berke JD (2019) Dissociable dopamine dynamics for learning and motivation. Nature 570:65–70.

Moorman DE, Aston-Jones G (2010) Orexin/hypocretin modulates response of ventral tegmental dopamine neurons to prefrontal activation: diurnal influences. J Neurosci 30:15585–15599.

Moritz AE, Foster JD, Gorentla BK, Mazei-Robison MS, Yang JW, Sitte HH, Blakely RD, Vaughan RA (2013) Phosphorylation of dopamine transporter serine 7 modulates cocaine analog binding. J Biol Chem 288:20–32.

Moron JA, Zakharova I, Ferrer JV, Merrill GA, Hope B, Lafer EM, Lin ZC, Wang JB, Javitch JA, Galli A, Shippenberg TS (2003) Mitogen-activated protein kinase regulates dopamine transporter surface expression and dopamine transport capacity. J Neurosci 23:8480–8488.

Muschamp JW, Dominguez JM, Sato SM, Shen RY, Hull EM (2007) A role for hypocretin (orexin) in male sexual behavior. J Neurosci 27:2837–2845.

Muschamp JW, Hollander JA, Thompson JL, Voren G, Hassinger LC, Onvani S, Kamenecka TM, Borgland SL, Kenny PJ, Carlezon WA Jr (2014) Hypocretin (orexin) facilitates reward by attenuating the antireward effects of its cotransmitter dynorphin in ventral tegmental area. Proc Natl Acad Sci USA 111:E1648–E1655.

Musnier A, Blanchot B, Reiter E, Crépieux P (2010) GPCR signalling to the translation machinery. Cell Signal 22:707–716.

Norregaard L, Frederiksen D, Nielsen EO, Gether U (1998) Delineation of an endogenous zinc-binding site in the human dopamine transporter. EMBO J 17:4266–4273.

O'Brien CP, Gardner EL (2005) Critical assessment of how to study addiction and its treatment: human and non-human animal models. Pharmacol Ther 108:18–58.

Oleson EB, Richardson JM, Roberts DC (2011) A novel IV cocaine self-administration procedure in rats: differential effects of dopamine, serotonin, and GABA drug pre-treatments on cocaine consumption and maximal price paid. Psychopharmacology 214:567–577.

Pignatelli M, Bonci A (2015) Role of dopamine neurons in reward and aversion: a synaptic plasticity Perspective. Neuron 86:1145–1157.

Richardson BD, Saha K, Krout D, Cabrera E, Felts B, Henry LK, Swant J, Zou MF, Newman AH, Khoshbouei H (2016) Membrane potential shapes regulation of dopamine transporter trafficking at the plasma membrane. Nat Commun 7:10423.

Robarge MJ, Agoston GE, Izenwasser S, Kopajtic T, George C, Katz JL, Newman AH (2000) Highly selective chiral N-substituted 3alpha-[bis(4′-fluorophenyl)methoxy]tropane analogues for the dopamine transporter: synthesis and comparative molecular field analysis. J Med Chem 43:1085–1093.

Roberts DC, Corcoran ME, Fibiger HC (1977) On the role of ascending catecholaminergic systems in intravenous self-administration of cocaine. Pharmacol Biochem Behav 6:615–620.

Roberts DC (2005) Preclinical evidence for GABAB agonists as a pharmacotherapy for cocaine addiction. Physiol Behav 86:18–20.

Roncero C, Ros-Cucurull E, Daigre C, Casas M (2012) Prevalence and risk factors of psychotic symptoms in cocaine-dependent patients. Actas Esp Psiquiatr 40:187–197.

Roy S (2014) Seeing the unseen: the hidden world of slow axonal transport. Neuroscientist 20:71–81.

Runegaard AH, Sorensen AT, Fitzpatrick CM, Jorgensen SH, Petersen AV, Hansen NW, Weikop P, Andreasen JT, Mikkelsen JD, Perrier JF, Woldbye D, Rickhag M, Wortwein G, Gether U (2018) Locomotor- and reward-enhancing effects of cocaine are differentially regulated by chemogenetic stimulation of Gi-signaling in dopaminergic neurons. eNeuro 5:ENEURO.0345-17.2018.

Salamone JD, Koychev I, Correa M, McGuire P (2015) Neurobiological basis of motivational deficits in psychopathology. Eur Neuropsychopharmacol 25:1225–1238.

Schmitt KC, Reith ME (2010) Regulation of the dopamine transporter: aspects relevant to psychostimulant drugs of abuse. Ann NY Acad Sci 1187:316–340.

Siciliano CA, Jones SR (2017) Cocaine potency at the dopamine transporter tracks discrete motivational states during cocaine self-administration. Neuropsychopharmacology 42:1893–1904.

Siciliano CA, Saha K, Calipari ES, Fordahl SC, Chen R, Khoshbouei H, Jones SR (2018) Amphetamine reverses escalated cocaine intake via restoration of dopamine transporter conformation. J Neurosci 38:484–497.

Sonders MS, Zhu SJ, Zahniser NR, Kavanaugh MP, Amara SG (1997) Multiple ionic conductances of the human dopamine transporter: the actions of dopamine and psychostimulants. J Neurosci 17:960–974.

Stuber GD, Hopf FW, Tye KM, Chen BT, Bonci A (2010) Neuroplastic alterations in the limbic system following cocaine or alcohol exposure. Curr Top Behav Neurosci 3:3–27.

Swanson LW (1998) Brain maps: structure of the rat brain. Amsterdam: Elsevier.

Tye KM, Mirzabekov JJ, Warden MR, Ferenczi EA, Tsai HC, Finkelstein J, Kim SY, Adhikari A, Thompson KR, Andalman AS, Gunaydin LA, Witten IB, Deisseroth K (2013) Dopamine neurons modulate neural encoding and expression of depression-related behaviour. Nature 493:537–541.

Ubersax JA, Ferrell JE Jr (2007) Mechanisms of specificity in protein phosphorylation. Nat Rev Mol Cell Biol 8:530–541.

Ungless MA, Singh V, Crowder TL, Yaka R, Ron D, Bonci A (2003) Corticotropin-releasing factor requires CRF binding protein to potentiate NMDA receptors via CRF receptor 2 in dopamine neurons. Neuron 39:401–407.

Volkow ND, Morales M (2015) The brain on drugs: from reward to addiction. Cell 162:712–725.

Volkow ND, Wise RA, Baler R (2017) The dopamine motive system: implications for drug and food addiction. Nat Rev Neurosci 18:741–752.

Werkman TR, McCreary AC, Kruse CG, Wadman WJ (2011) NK3 receptors mediate an increase in firing rate of midbrain dopamine neurons of the rat and the guinea pig. Synapse 65:814–826.

Wise RA, Newton P, Leeb K, Burnette B, Pocock D, Justice JB Jr (1995) Fluctuations in nucleus accumbens dopamine concentration during intravenous cocaine self-administration in rats. Psychopharmacology 120:10–20.

Witten IB, Steinberg EE, Lee SY, Davidson TJ, Zalocusky KA, Brodsky M, Yizhar O, Cho SL, Gong S, Ramakrishnan C, Stuber GD, Tye KM, Janak PH, Deisseroth K (2011) Recombinase-driver rat lines: tools, techniques, and optogenetic application to dopamine-mediated reinforcement. Neuron 72:721–733.

Woodward JJ, Wilcox RE, Leslie SW, Riffee WH (1986) Dopamine uptake during fast-phase endogenous dopamine release from mouse striatal synaptosomes. Neurosci Lett 71:106–112.

Yorgason JT, España RA, Jones SR (2011) Demon voltammetry and analysis software: analysis of cocaine-induced alterations in dopamine signaling using multiple kinetic measures. J Neurosci Methods 202:158–164.

Zou MF, Cao J, Abramyan AM, Kopajtic T, Zanettini C, Guthrie DA, Rais R, Slusher BS, Shi L, Loland CJ, Newman AH (2017) Structure-activity relationship studies on a series of 3alpha-[bis(4-fluorophenyl)methoxy]tropanes and 3alpha-[bis(4-fluorophenyl)methylamino]tropanes as novel atypical dopamine transporter (DAT) inhibitors for the treatment of cocaine use disorders. J Med Chem 60:10172–10187.